Interference Mitigation for Dynamic TDD Networks Employing Sounding Signals

Darlan C. Moreira, Lászlon R. Costa, Yuri C. B. Silva and Igor M. Guerreiro

***Abstract*—The requirements of fifth-generation (5G) mobile communications include services with low delay and high throughput. Network densification is pointed to as a promising method to increase the network capacity. However, this solution brings new problems, such as the fast variation in traffic demands among access nodes (ANs) and between uplink and downlink, leading to high delays. To solve the traffic issues in dense networks, dynamic time division duplex (DTDD) is pointed as a possible solution. This strategy creates a new kind of interference between ANs and user equipments (UEs) called cross-interference. Therefore, obtaining channel state information (CSI) of cross-interference channels is essential for implementing interference mitigation methods, such as interference alignment, coordinated beamforming, resource schedulers, among others. Hence, this work proposes methods to estimate the intended and interfering channels based on sounding reference signal (SRS) and/or demodulation reference signal (DMRS). A coordinated scheme is developed to assign sounding signals in the network and reduce the interference perceived during the channel sounding, which improves the channel estimation quality. Furthermore, a refined successive interference cancellation (SIC) algorithm is proposed for estimating the channel. To assess system performance, a zero-forcing beamforming algorithm has been developed based on the CSI acquired with the proposed methods. This algorithm handles the degrees of freedom issues when ANs are operating in opposite directions. The numerical results show that the improved channel quality provided by the proposed estimation algorithm increases network capacity.**

***Index Terms*—Dynamic TDD, Interference Management, Channel Sounding.**

I. Introduction

Due to the densification of communication networks and the advent of smaller cells, interference is often the main problem to be overcome [1]. The access nodes (ANs) can perform effective interference mitigation, such as smart scheduling and/or coordinated beamforming, if they consider some channel state information (CSI) from the intended and interfering channels.

In general, mobile networks operate in half-duplex separating the uplink/downlink transmissions through frequency division duplex (FDD) or time division duplex (TDD). In FDD, different bands of spectrum are allocated for uplink and downlink transmission at the same time, while in TDD the same spectrum is used for both transmission directions in different time slots. Therefore, TDD can exploit the complete bandwidth available to each direction and accommodate downlink/uplink traffic asymmetry by shrinking the transmission time of each direction following traffic demands.

In dense networks, the downlink/uplink instantaneous traffic demands have fast fluctuation due to the small number of user equipments (UEs) associated with each AN. In static TDD, the ANs follow some set of pre-defined uplink/downlink subframe configurations, where all ANs in the network follow the same configuration [2]. In this method, some ANs may operate in an unsuitable uplink/downlink proportion, thus increasing network latency. In dynamic time division duplex (DTDD), each AN is independent do decide the uplink/downlink directions to accommodate its traffic demands. Therefore, DTDD can improve spectrum usage and reduce network latency.

Due to the flexibility of neighbor ANs operating in different transmission directions (downlink or uplink) at the same time in DTDD systems, mitigating interference is even more important. There are two types of interference in a DTDD network: the co-channel interference which comes from transmissions in the same link direction, and the cross-channel interference, from transmissions in opposite link directions. The interference coming from those different types of sources in DTDD systems complicates obtaining the CSI, due to the interfering sounding signals sent by other ANs and their UEs.

A typical DTDD scenario is shown in Figure 1, where one cell is in the downlink direction and the other cell is in the uplink direction, each cell serving one UE.

The sounding reference signal (SRS) and demodulation reference signal (DMRS) are important reference signals in long term evolution (LTE) systems [3], as well as in fifth-generation (5G) systems [4]. These sounding signals are based on constant amplitude zero autocorrelation (CAZAC) sequences, which are

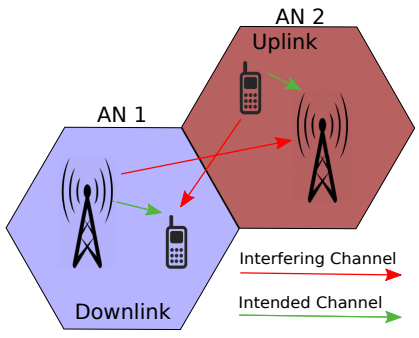

Figure 1. Typical DTDD scenario.

This work was supported by Ericsson Research, Sweden, and Ericsson Innovation Center, Brazil, under EDB/UFC.42 and EDB/UFC.45 Technical Cooperation Contracts. This work was financed in part by the Coordenação de Aperfeiçoamento de Pessoal de Nível Superior - Brasil (CAPES) - Finance Code 001, CAPES/PRINT Proc. no. 88887.311965/2018-00. Darlan Moreira and Lászlon Costa would like to acknowledge CAPES for the scholarship support. Yuri C. B. Silva also acknowledges the support of CNPq.

The authors are with the Wireless Telecommunications Research Group (GTEL), Federal University of Ceará (UFC), Fortaleza, Ceará, Brazil (e-mail: {darlan,laszlon,yuri,igor}@gtel.ufc.br).

Digital Object Identifier: 10.14209/jcis.2020.32

generated as described in [4]. The main goal of SRS is to allow the AN to estimate the uplink channel in frequency resources unused by the UE, to support channel dependent resource scheduling. On the other hand, the DMRS is sent jointly with data in scheduled frequency resources to support coherent demodulation. Both signals are used to get CSI and they are the focus of this work.

Considering a TDD system, where channel reciprocity can be assumed, the SRS also allows the AN to make better decisions for the downlink channel. One such example is using the SRS sequences sent by the UEs from different ANs to infer how much interference an AN would cause to unintended UEs, as demonstrated in [5]. Based on this information, the ANs can design beamforming, scheduling, and power allocation to reduce the overall interference in the system.

There are many proposals in the literature to improve channel estimation quality or functionalities of the network using SRS. In [6], the SRS is used to estimate the UE to UE channel to detect potential candidates for performing device-to-device communication. In [7], SRS is used to estimate the path loss and relative channel status to aid downlink scheduling in TDD systems. In [8] and [9] methods to handle the limited number of orthogonal SRS sequences in a massive multiple-input multiple-output (MIMO) scenario are proposed. In [8] the authors proposed to create groups of UEs with high correlated channels in a massive MIMO scenario. Therefore, the use of orthogonal SRS sequences can be reduced since it is not necessary to sound the channels of all UEs in a group to acquire CSI. In [9], the authors proposed a dynamic reuse method to assign the orthogonal SRS sequences in a massive MIMO network reducing pilot contamination.

When considering the knowledge of interfering channels it becomes possible to efficiently calculate precoders and decoders to mitigate the interference. Many works in the literature consider such knowledge to design transceivers to control the co-channel and cross-channel interference in DTDD networks [10]–[13]. This represents a practical issue since SRS and DMRS were not originally designed to estimate the cross-channels.

In [5], [14], [15], methods to mitigate the inter-cell interference using SRS to acquire interfering CSI are evaluated. In [14], a weighted sum rate optimization problem is proposed to design precoders based on uplink sounding signals and channel reciprocity. The authors consider that all ANs in the network know the sounding signals sent by UEs in an uplink transmission and use this information to get the CSI for all UEs in the network. However, the authors did not show results concerning the channel estimation quality of the employed methods, so that the CSI reliability cannot be verified for a practical system. In [15] the authors propose a decentralized solution for downlink interference mitigation that explores the channel reciprocity in a TDD network. In the proposed method, base stations estimate the interference covariance matrix obtained from a preceding version of SRS transmitted in the uplink. For this, the authors consider that all UEs are transmitting at the same time. The main drawback of this approach is the added overhead in the system. To mitigate the overhead problems, the authors in [5] analyze a method where UEs precode the SRS to inform their own ANs and interfering ANs the desired subspace for the received signal. The subspace selection and precoded sounding made by UEs is based on the interference from a previous downlink transmission or on the CSI of the intended channel, which can reduce the overhead in the network.

In this work, we investigate the quality of channel estimation using a proposed refined successive interference cancellation (SIC) algorithm, as well as a coordinated sounding signal assignment for DTDD systems. To the best of our knowledge there is no previous study of sounding and channel estimation for DTDD systems. Our proposals are based on new radio (NR) channel sounding and could also be applied to LTE legacy networks. The main contributions of this work are:

1) A refined SIC algorithm that can significantly improve the quality of the estimated channels in a multi-cell network and allow estimating the interfering channels[1];
2) A method to coordinate the reference sounding signal assignment among ANs to improve the channel estimation quality and reduce the complexity of the channel estimation;

The rest of this paper is organized as follows. Section II describes the system model for the DTDD scenario, as well as the signal-to-interference-plus-noise ratio (SINR) model considered in this work. Section III describes the proposed and adopted channel estimation methods. In Section IV the sounding signal assignment algorithms are described. The zero-forcing beamforming is presented in Section V. Section VI shows some simulation results and demonstrates the channel estimation quality considering the capacity gains with the proposed methods. Finally, Section VII presents the main conclusions of this work.

In this article the following notation is adopted: Upper/lower boldface letters are used for matrices/vectors. The operators $(\cdot)^{\mathrm{T}}$, $(\cdot)^{\mathrm{H}}$ and $|\cdot|$ indicate, respectively, the transpose, complex conjugate transpose, and absolute value of the corresponding argument. The indexes m and p are used for different ANs. Similarly, the indexes k and b denote different UEs. The symbol $\leftarrow$ represents uplink direction and is used to distinguish between uplink and downlink precoders, decoders and channels.

II. System Model

In this work, we consider a cooperative cluster with M ANs, where the mth AN is serving a set of $\mathcal{K}_m$ UEs. The cooperative cluster works in DTDD mode, where each cell can operate either in uplink or in downlink direction.

The system model is a multi-user (MU)-MIMO scenario, where UE $k \in \mathcal{K}_m$ has N_k antennas and the AN m has N_m antennas. In a given AN, multiple UEs can transmit/receive signals at the same time, which are separated through space division multiple access (SDMA).

[1]The interfering channels are often weaker than the desired channel and thus suffer heavy interference from the desired channel during the channel estimation.

Let $\mathcal{U}$ denote the set of ANs in the uplink and $\mathcal{D}$ the set of ANs in the downlink. The signal received by an AN m in the uplink direction is given by:

$$\overleftarrow{\mathbf{y}}_m = \underbrace{\sum_{k\in\mathcal{K}_m} \overleftarrow{\mathbf{H}}_{m,(m,k)} \overleftarrow{\mathbf{W}}_{m,k} \overleftarrow{\mathbf{x}}_{m,k}}_{\text{Intended Signal}} + \underbrace{\sum_{p\in\mathcal{U}\setminus m} \sum_{b\in\mathcal{K}_p} \overleftarrow{\mathbf{H}}_{m,(p,b)} \overleftarrow{\mathbf{W}}_{p,b} \overleftarrow{\mathbf{x}}_{p,b}}_{\text{Co-Channel Interference}} + \underbrace{\sum_{p\in\mathcal{D}} \sum_{b\in\mathcal{K}_p} \mathbf{H}_{m,p}\mathbf{W}_{p,b}\mathbf{x}_{p,b}}_{\text{Cross-Channel Interference (from downlink ANs)}} + \underbrace{\mathbf{n}_m}_{\text{additive noise}}, \quad (1)$$

where $\mathbf{n}_m \sim \mathcal{CN}(0,\sigma^2)$ denotes the additive noise at AN m with zero mean and variance σ^2 and $\overleftarrow{\mathbf{H}}_{a,(b,k)}$ is the uplink channel matrix from UE $k \in \mathcal{K}_b$ to AN a (that is, from UE k served by AN b to AN a), which has dimension $N_a \times N_k$. The $\mathbf{H}_{m,p}$ term denotes a cross-channel matrix from AN p to AN m, which has dimension $N_m \times N_p$. The matrix $\overleftarrow{\mathbf{W}}_{m,k}$ is the uplink precoder used by UE $k \in \mathcal{K}_m$ to send a signal vector $\overleftarrow{\mathbf{x}}_{m,k}$. The precoder has dimension $N_k \times d_k$, where d_k is the number of transmit streams, and the signal vector has dimension $d_k \times 1$. Similarly, the downlink precoder $\mathbf{W}_{p,k}$ is used by the pth AN to send the signal vector $\mathbf{x}_{p,k}$ to a UE $k \in \mathcal{K}_p$. In this case, the precoder dimension is $N_p \times d_k$ and the signal vector has dimension $d_k \times 1$.

The signal received in the downlink direction by a UE $k \in \mathcal{K}_m$ is given by:

$$\mathbf{y}_{m,k} = \underbrace{\mathbf{H}_{m,(m,k)}\mathbf{W}_{m,k}\mathbf{x}_{m,k}}_{\text{Intended Signal}} + \underbrace{\sum_{b\in\mathcal{K}_m\setminus k} \mathbf{H}_{m,(m,b)}\mathbf{W}_{m,b}\mathbf{x}_{m,b}}_{\text{Intra-cell Interference}} + \underbrace{\sum_{p\in\mathcal{D}\setminus m} \sum_{b\in\mathcal{K}_p} \mathbf{H}_{p,(m,k)}\mathbf{W}_{p,b}\mathbf{x}_{p,b}}_{\text{Co-channel Interference}} + \underbrace{\sum_{p\in\mathcal{U}} \sum_{b\in\mathcal{K}_p} \mathbf{H}_{(m,k),(p,b)} \overleftarrow{\mathbf{W}}_{p,b} \overleftarrow{\mathbf{x}}_{p,b}}_{\text{Cross-channel Interference (from uplink UEs)}} + \underbrace{\mathbf{n}_{m,k}}_{\text{addtive noise}}, \quad (2)$$

where $\mathbf{n}_{m,k} \sim \mathcal{CN}(0,\sigma^2)$ denotes the additive noise at UE k and $\mathbf{H}_{(m,k),(p,b)}$ is the channel between UE $k \in \mathcal{K}_m$ and UE $p \in \mathcal{K}_b$. Each column of the transmission matrices $\mathbf{W}_{m,k}$ and $\overleftarrow{\mathbf{W}}_{m,k}$ are transmission vectors of the corresponding streams. Let $\mathbf{w}_{m,k}^{[q]}$ and $\overleftarrow{\mathbf{w}}_{m,k}^{[q]}$ be the transmission vectors of stream q of UE $k \in \mathcal{K}_m$ in the downlink and uplink direction. Let the vectors $\mathbf{u}_{m,k}^{[q]}$ and $\overleftarrow{\mathbf{u}}_{m,k}^{[q]}$ be the receive filters of stream q of UE $k \in \mathcal{K}_m$ in the downlink and uplink direction, respectively. The uplink SINR is then given by:

$$\overleftarrow{\gamma}_{m,k}^{[q]} = \frac{\overleftarrow{\mathbf{u}}_{m,k}^{[q]\,\mathrm{H}} \overleftarrow{\mathbf{H}}_{m,(m,k)} \overleftarrow{\mathbf{w}}_{m,k}^{[q]} \left(\overleftarrow{\mathbf{w}}_{m,k}^{[q]}\right)^{\mathrm{H}} \overleftarrow{\mathbf{H}}_{m,(m,k)}^{\mathrm{H}} \overleftarrow{\mathbf{u}}_{m,k}^{[q]}}{\left(\overleftarrow{\mathbf{u}}_{m,k}^{[q]}\right)^{\mathrm{H}} \overleftarrow{\mathbf{B}}_{m,k}^{[q]} \overleftarrow{\mathbf{u}}_{m,k}^{[q]}}, \quad (3)$$

where the matrix $\overleftarrow{\mathbf{B}}_{m,k}^{[q]}$ is the uplink interference plus noise matrix given by:

$$\overleftarrow{\mathbf{B}}_{m,k}^{[q]} = \underbrace{\sum_{\substack{v=1\\v\neq q}}^{d_{k\in\mathcal{K}_m}} \overleftarrow{\mathbf{H}}_{m,(m,k)} \overleftarrow{\mathbf{w}}_{m,k}^{(v)} \left(\overleftarrow{\mathbf{w}}_{m,k}^{(v)}\right)^{\mathrm{H}} \overleftarrow{\mathbf{H}}_{m,(m,k)}^{\mathrm{H}}}_{\text{Inter-Layer Interference}} + \underbrace{\sum_{b\in\mathcal{K}_m\setminus k} \sum_{q=1}^{d_b} \overleftarrow{\mathbf{H}}_{m,(m,b)} \overleftarrow{\mathbf{w}}_{m,b}^{[q]} \left(\overleftarrow{\mathbf{w}}_{m,b}^{[q]}\right)^{\mathrm{H}} \overleftarrow{\mathbf{H}}_{m,(m,b)}^{\mathrm{H}}}_{\text{Intra-Cell Interference}} + \underbrace{\sum_{p\in\mathcal{U}\setminus m} \sum_{b\in\mathcal{K}_p} \sum_{q=1}^{d_b} \overleftarrow{\mathbf{H}}_{m,(p,b)} \overleftarrow{\mathbf{w}}_{p,b}^{[q]} \left(\overleftarrow{\mathbf{w}}_{p,b}^{[q]}\right)^{\mathrm{H}} \overleftarrow{\mathbf{H}}_{m,(p,b)}^{\mathrm{H}}}_{\text{Inter-Cell Interference (Co-Channel Interference)}} + \underbrace{\sum_{p\in\mathcal{D}} \sum_{b\in\mathcal{K}_p} \sum_{q=1}^{d_b} \mathbf{H}_{m,p}\mathbf{w}_{p,b}^{[q]} \left(\mathbf{w}_{p,b}^{[q]}\right)^{\mathrm{H}} \mathbf{H}_{m,p}^{\mathrm{H}}}_{\text{Inter-Cell Interference (Cross-Channel Interference)}} + \underbrace{\sigma_m \mathbf{I}_{N_m}}_{\text{Noise}}, \quad (4)$$

with σ_m representing the noise power at AN m.

Similarly, the downlink SINR of a stream q of a UE $k \in \mathcal{K}_m$ is given by:

$$\gamma_{m,k}^{[q]} = \frac{\left(\mathbf{u}_{m,k}^{[q]}\right)^{\mathrm{H}} \mathbf{H}_{m,(m,k)} \mathbf{w}_{m,k}^{[q]} \left(\mathbf{w}_{m,k}^{[q]}\right)^{\mathrm{H}} \mathbf{H}_{m,(m,k)}^{\mathrm{H}} \mathbf{u}_{m,k}^{[q]}}{\left(\mathbf{u}_{m,k}^{[q]}\right)^{\mathrm{H}} \mathbf{B}_{m,k}^{[q]} \mathbf{u}_{m,k}^{[q]}}, \quad (5)$$

where the downlink interference plus noise matrix of a stream q of an AN $k \in \mathcal{K}_m$ is defined as:

$$\mathbf{B}_{m,k}^{[q]} = \underbrace{\sigma_k \mathbf{I}_{N_k}}_{\text{Noise}} + \underbrace{\sum_{\substack{v=1\\v\neq q}}^{d_k} \mathbf{H}_{m,(m,k)} \mathbf{w}_{m,k}^{(v)} \left(\mathbf{w}_{m,k}^{(v)}\right)^{\mathrm{H}} \mathbf{H}_{m,(m,k)}^{\mathrm{H}}}_{\text{Inter-Layer Interference}} + \underbrace{\sum_{b\in\mathcal{K}_m\setminus k} \sum_{q=1}^{d_b} \mathbf{H}_{m,(m,b)} \mathbf{w}_{m,b}^{[q]} \left(\mathbf{w}_{m,b}^{[q]}\right)^{\mathrm{H}} \mathbf{H}_{m,(m,b)}^{\mathrm{H}}}_{\text{Intra-Cell Interference}} + \underbrace{\sum_{p\in\mathcal{D}\setminus m} \sum_{b\in\mathcal{K}_p} \sum_{q=1}^{d_b} \mathbf{H}_{p,(m,k)} \mathbf{w}_{p,b}^{[q]} \left(\mathbf{w}_{p,b}^{[q]}\right)^{\mathrm{H}} \mathbf{H}_{p,(m,k)}^{\mathrm{H}}}_{\text{Inter-Cell Interference (Co-Channel Interference)}} + \underbrace{\sum_{p\in\mathcal{U}} \sum_{b\in\mathcal{K}_p} \sum_{q=1}^{d_b} \mathbf{H}_{(m,k),(p,b)} \overleftarrow{\mathbf{w}}_{p,b}^{[q]} \left(\overleftarrow{\mathbf{w}}_{p,b}^{[q]}\right)^{\mathrm{H}} \mathbf{H}_{(m,k),(p,b)}^{\mathrm{H}}}_{\text{Inter-Cell Interference (Cross-Channel Interference)}}, \quad (6)$$

with σ_k representing the noise power at user k.

Note that the SINRs described in (3) and (5) are dependent on receiving filters and interfering/intended precoders. Therefore, proper channel estimation of the interferers is important in spatial filter design.

In the next section, we present a new channel estimation method using standard LTE and NR signals for a DTDD scenario where the interfering channels can also be estimated.

III. The Iterative SIC Algorithm

In this section, we describe the proposed iterative SIC algorithm which improves a channel estimation algorithm from the literature [5], [16]. The original algorithm in [16] takes advantage of the orthogonal frequency division multiplexing (OFDM) structure and the CAZAC properties[2] of the reference sequences to separate the channel impulse response (CIR) of the different layers (from the same UE and/or different UEs).

For illustration purposes, let us employ SRS sequences, considering that the process is similar when DMRS sequences are employed. SRS and DMRS are defined in long term evolution - advanced (LTE-A) and NR standards [3], [4]. An SRS sequence $r_u^{(\alpha)}(n)$ is defined by a cyclic shift (CS) α of a base sequence $\bar{r}_u(n)$ according to

$$r_u^{(\alpha)}(n) = e^{j\alpha n} \cdot \bar{r}_u(n), \quad 0 \le n < \text{EZC}, \tag{7}$$

where EZC[3] is the length of the reference signal. The base sequence is defined as a cyclic extension of a Zadoff-Chu sequence [17], that is

$$\bar{r}_u(n) = x_q(n \mod N_{\text{ZC}}), \quad 0 \le n < \text{EZC} \tag{8}$$

$$x_q(l) = e^{\frac{\pi q m(m+1)}{N_{\text{ZC}}}}, \quad 0 \le m < N_{\text{ZC}} - 1, \tag{9}$$

where $x_q(l)$ is the qth root Zadoff-Chu sequence and N_{ZC} is the size of the original Zadoff-Chu sequence, given by the largest prime number such that $N_{\text{ZC}} < \text{EZC}$. The CS value α is given by $\alpha = 2\pi n_{cs}/N_{cs}$ where N_{cs} is the total number of cyclic shifts and n_{cs} can assume (integer) values from 0 to $N_{cs} - 1$. In 5G NR it is possible to consider 8 or 12 cyclic shifts for SRS in accordance with the number of comb patterns [4], thus, there are N_{cs} possible values of α in total, represented by the small numbers inside the circle in Figure 2. However, not necessarily all possible values for

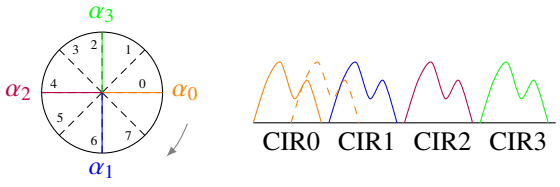

Figure 2. Cyclic Shifts

n_{cs} will be used, with the channel memory limiting which n_{cs} values can be employed. As an example, consider a case where four reference sequences, which share the same root sequence but have different α values ($\alpha_0, \alpha_1, \alpha_2$ and α_3), were sent. If we multiply the received signal by the conjugate of the root sequence we get a concatenation of the CIRs, as depicted in Figure 2 with the solid lines. If an additional sequence were sent with an α value obtained with $n_{cs} = 1$ we would get the dashed CIR in Figure 2, which would interfere with CIR0 and CIR1 during the channel estimation. On the other hand, if the channel memory was smaller, we would be able to use all cyclic shifts for the same root sequence and still completely separate the CIRs. At last, note that any reference signal using a different root sequence would cause interference in all CIRs in Figure 2, independently of the employed cyclic shift.

In summary, to estimate the channel from a UE, the AN needs to multiply element-wise the received signal in the frequency domain by the conjugate of the UE's reference signal. Afterward, it must apply an inverse fast Fourier transform (IFFT) to go to the time domain and obtain the concatenated CIR[4] of all UE layers. Then, it can zero out any component above some delay (the expected channel memory) and apply a fast Fourier transform (FFT) to get the estimated channel in the frequency domain.

When multiple reference signals are sent that do not share the same root sequence, then interference in the channel estimation process is inevitable. One way to mitigate this interference is through a successive interference cancellation approach, where any previously detected signal's contribution is removed from the received signal such that subsequent detection has less interference. One problem that can happen with a successive interference cancellation approach is the error propagation, which occurs if a signal is wrongly detected and then subtracted to remove its contribution. If a signal is wrongly detected then the removal of its contribution from the total received signal is also incorrect and, instead of having less interference after the removal, the remaining total signal is now distorted. To mitigate this problem, one should first detect the strongest signal, remove its contribution, detect the next strongest signal, and so on. The SIC algorithm is summarized in Algorithm 1.

Algorithm 1 SIC channel estimation for a given AN j.

1: Create a pool $\mathcal{I}$ of channel links to estimate: $i \subset \mathcal{I}$ $\forall i$
2: **repeat**
3: Estimate all channel links in $\mathcal{I}$ independently using the previously described regular channel estimation [5], [16]
4: Select the estimated channel link $i^* \in \mathcal{I}$ that has the largest norm
5: Remove the link i^* component (the estimated channel times the corresponding reference signal) from the received signal
6: Remove i^* from $\mathcal{I}$
7: **until** $\mathcal{I}$ is empty

In Algorithm 1 the problem of error propagation is reduced, but a remaining problem is that the first signals suffer from more interference than the last signals, since more interference has been removed when the later signals are detected. To improve this we have proposed an iterative SIC algorithm, where after detecting all signals as described in Algorithm 1 we "re-detect" all signals again in the same order. The "re-detection" of the signals is performed digitally considering the already received signals. That means that we can detect all signals again, but since we have an initial estimation for all channels we can remove the contribution from all signals except the desired one from the received signal. The iterative algorithm is summarized in Algorithm 2.

[2]The SRS and DMRS reference signals are both CAZAC signals.

[3]The root sequence is an extension of a Zadoff-Chu sequence and we denote EZC as the size of the extended sequence.

[4]The desired UE's signal is always the first one since we multiplied the received signal by that UE's sequence.

Algorithm 2 Refined SIC channel estimation for AN j.

1: Obtain an initial channel estimation with Algorithm 1 and save the order the channels were estimated in a list $\mathbf{o}$
2: **repeat**
3: Define the auxiliary list as $\overline{\mathbf{o}} = \mathbf{o}$
4: **repeat**
5: Select the first channel i^* from the list $\overline{\mathbf{o}}$ and remove the interfering signals of all other channels.
6: Update the estimated channel for the i^*th link applying the regular channel estimation, but now with a received signal "free" from the interference of all other reference signals
7: Remove i^* from the list $\overline{\mathbf{o}}$
8: **until** The list is empty
9: **until** Convergence

In this work, we consider that the AN has enough computational resources to conclude all iterations of the algorithm before the next transmission time. Therefore, the proposed algorithm does not increase transmission latency. Since each iteration improves the quality of the estimated channels, it is also possible to perform fewer iterations to reduce complexity, if necessary, while still benefiting from the algorithm.

IV. Multi-Cell Reference Signals Assignment

The SRS and DMRS have the property that two sequences are orthogonal if they have both the same root sequence but different cyclic shifts. Furthermore, two sequences are also orthogonal if they employ different orthogonal cover codes (OCCs) (in the case of DMRS) or comb patterns (in the case of SRS). In this section, we present generic algorithms for DMRS and SRS sequence assignment. However, for simplicity only the algorithms for SRS are presented. Note that these signal distribution methods can be applied with DMRS as well, with the only change being that coordinating OCC allocation is performed instead of coordinating the comb pattern.

We have investigated the following methods to allocate the sounding sequences:

- **DMRS/SRS**: This method is similar to how the DMRS/SRS sequences are allocated in LTE-A [3] and NR [4]. In this approach, each AN has its root sequence and distributes the orthogonal signals (DMRS or SRS sequences corresponding to the root sequence with different comb patterns[5] and cyclic shifts) without any coordination between neighbor cells. Each AN has its root sequences and distributes the cyclic shifts among its UE streams.
- **Coordinated-DMRS/SRS**: This method corresponds to the maximum coordination along with the network when allocating the sounding resources. The DMRS or SRS configuration aims at maximizing the number of interfering users allocated to the same root sequence, but with different comb patterns and cyclic shifts. That is, in this case, different ANs might employ the same root sequence and coordinate the allocation of different cyclic shifts/comb patterns[6] to their UEs. Thus, this method leads to less interference than DMRS/SRS-LTE.

To avoid the impact of inter-layer interference, the allocation of the sounding sequences in the multi-stream case gives priority to orthogonalizing signals from the same UE. Let $\mathbf{c_{cs}}$ be a vector containing all cyclic shifts to be applied to a root sequence, and $\mathbf{r}_k$ a vector with root sequences available to AN k. The **SRS** method is described in Algorithm 3. In summary, the SRS varies the comb pattern index first, followed by the cyclic shift index of the same root sequence, and only then changes to a different root sequence.

Algorithm 3 SRS for a given AN k.

Require: σ_k, $\mathbf{r}_k$
1: Initialize $cs\_count \leftarrow 1$ and $cp \leftarrow 1$
2: **for** $n \leftarrow 1$ **to** σ_k **do** {Loop for each stream}
3: Allocate the first root sequence of $\mathbf{r}_k$ to stream n
4: Allocate $\mathbf{c_{cs}}[cs\_count]$ to stream n
5: Allocate cp to stream n
6: **if** $cp = 1$ **then** {Go to second Comb Pattern}
7: $cp \leftarrow 2$
8: **else** {Go back to the first Comb Pattern}
9: $cp \leftarrow 1$
10: **if** $cs\_count < length(\mathbf{c_{cs}})$ **then**
11: $cs\_count \leftarrow cs\_count + 1$
12: **else**
13: $cs\_count \leftarrow 1$
14: Remove the first root sequence of $\mathbf{r}_k$
15: **end if**
16: **end if**
17: **end for**

The values cs_count and cp are the cyclic shift counter and the comb pattern index to be allocated to stream n. The first step of the algorithm is the initialization of the cyclic shift and comb pattern, which will be allocated to the first stream. The loop from line 2 to line 17 allocates the sounding resource to all σ_k streams of the UE in AN k. In steps 3 to 4 the current available sounding resource is allocated to stream n. Steps from 6 to 16 determine what is the next available sounding resource to be allocated to the next stream. If we are in the first comb pattern (from 2 available comb patterns), then just change the cp to 2 while keeping the same root sequence and cyclic shift index. Otherwise, change cp back to 1 (it would be 2 in this case) and change to the next available cyclic shift of the same root sequence. If we are already in the last cyclic shift of a root sequence, then change cs_count back to 1 and go to the next root sequence.

Note that the same cyclic shift is allocated two times consecutively so that the comb pattern is used to mitigate the intra-stream interference. The motivation is that the comb pattern orthogonalization is more robust to mitigate interference than different cyclic shifts, since the latter would not provide full orthogonalization if the channel delay spread is too large.

This algorithm is an extension of the algorithm used in LTE-A and NR to higher rank transmissions, considering that

[5]OCCs for DMRS.

[6]Cyclic shifts/OCCs for DMRS.

the highest transmission rank of the LTE-A pattern is of 4 streams.

At last, the fully-coordinated approach, Coordinated-SRS, coordinates the comb pattern, cyclic shift and root sequences distribution. Therefore, it is possible that more than one AN employs the same root sequence, but with different "cyclic shift/occ" pairs.

Let us consider a vector with all possible root sequences $\mathbf{r} = [\mathbf{r}_1^{\mathrm{T}}, \mathbf{r}_2^{\mathrm{T}}, \ldots, \mathbf{r}_K^{\mathrm{T}}]^{\mathrm{T}}$ and the number of orthogonal signals, *num_ort_sig*, which can be generated from a root sequence (*num_ort_sig* being equal to the number of possible cyclic shifts/OCC combinations). The Coordinated-SRS approach is then described in Algorithm 4.

Algorithm 4 Coordinated-SRS for the overall network.

Require: σ_k $\forall k$ and $\mathbf{r}$
1: Define $num\_ort\_sig \leftarrow 2 \cdot length(\mathbf{c_{cs}})$
2: Initialize $ort\_sig\_count \leftarrow 0$
3: Initialize $cp \leftarrow 1$
4: Initialize $cs\_count \leftarrow 1$
5: **for** $k \leftarrow 1$ **to** K **do** {Loop for each AN}
6: **if** $\sigma_k > num\_ort\_sig - ort\_sig\_count$ **then** {Use next root sequence if necessary}
7: Remove the first root sequence of $\mathbf{r}$
8: $cp \leftarrow 1$
9: $cs\_count \leftarrow 1$
10: $ort\_sig\_count \leftarrow 0$
11: **end if**
12: **for** $n \leftarrow 1$ **to** σ_k **do** {Loop for each stream}
13: Allocate the first root sequence of $\mathbf{r}$ to stream n
14: Allocate $\mathbf{c_{cs}}[cs\_count]$ to stream n
15: Allocate cp to stream n
16: $ort\_sig\_count \leftarrow ort\_sig\_count + 1$
17: **if** $cp = 1$ **then**
18: $cp \leftarrow 2$
19: **else**
20: $cp \leftarrow 1$
21: **if** $cs\_count < length(\mathbf{c_{cs}})$ **then**
22: $cs\_count \leftarrow cs\_count + 1$
23: **else**
24: $cs\_count \leftarrow 1$
25: Remove the first root sequence of $\mathbf{r}$
26: **end if**
27: **end if**
28: **end for**
29: **end for**

The value of *num_ort_sig* corresponds to twice the number of cyclic prefixes, since we have two comb patterns. This is calculated in line 1 of Algorithm 4. Lines 2 to 4 then initialize the counters (*ort_sig_count* being the number of orthogonal signals already allocated in the current root sequence). Afterwards, the loop from lines 5 to 29 allocates the sounding signals to each stream in the system.

To reduce the inter-layer interference, the Coordinated-SRS approach does not allocate signals generated from different root sequences to the same UE. Reference sequences generated from different root sequences are not fully orthogonalized even when they have different cyclic shifts. In Algorithm 4 this is performed from line 6 to line 11, where line 6 checks if the number of available orthogonal signals in the current root sequence is enough to serve all streams of UE k.

V. Beamforming For Interference Mitigation

By employing the channel estimation and reference signal assignment presented in Sections III and IV, the ANs in the uplink can estimate the channel between other ANs (in downlink) and UEs (in uplink).

The same estimation can be performed by UEs to get CSI between other UEs (in uplink) and ANs (in downlink), however, this estimation requires the UEs to know the reference signals sent in the cooperative cluster. The number of UE-to-UE cross-channels grows exponentially with the number of UEs in the cooperative network. Despite this, the cyclic shift and root sequence transmitted at each transmit time interval (TTI) must be shared among UEs, which may increase the network signaling, making it impractical for a realistic scenario. To reduce the signaling requirements, we consider in this work that the interference mitigation must be performed only for the ANs' transmission, thus avoiding the extra signaling to UEs. This practical assumption means that UEs' cross-interference will not be mitigated.

Note that the interfering UEs do not have a way to estimate the interfering channel. Therefore, the UEs take only the intended channel into account when choosing a suitable uplink beamforming filter. For that reason we consider the maximum ratio transmission (MRT), which maximizes the signal power at the receiver, as uplink precoder (performed by UEs). On the other hand, zero-forcing (ZF) based on singular value decomposition (SVD) is assumed as downlink precoder (performed by ANs). ZF is a well-known beamforming approach that nulls the interfering signals. While other beamforming methods may also fit in our proposed approach, maximizing the capacity through spatial filtering is not the focus of this work. Hence, ZF was chosen for the system-level evaluation.

In the scenario where there is some AN pair m in downlink and p in uplink with $N_m \leq N_p$, there are not enough degrees of freedom to perform ZF. For this case, we have to create an equivalent channel between ANs with a lower channel matrix rank, based on the range space of UEs. This rank reduction is possible if $N_{k \in \mathcal{K}_p} < N_m$, which is a reasonable assumption due to the increasing antennas trend of 5G systems.

In the following, we briefly describe the steps of Algorithm 5, which presents the DTDD ZF performed by each AN in the downlink.

In steps 1-2 of Algorithm 5, we compute the range space $\mathbf{V}^{(1)}_{p,(p,b)}$ of each UE b in uplink to create an equivalent channel, $\overline{\mathbf{H}}_{m,(p,b)}$, between the AN m in downlink and AN p.

Then, in the steps 3-7 we stack all interfering channels in the matrix $\widetilde{\mathbf{H}}_{m,(m,k)}$, which includes the equivalent channels created for uplink UEs, downlink UEs from different ANs and/or interfering UEs in the same cell m.

In step 8 the interference null space of a UE $k \in \mathcal{K}_m$, $\widetilde{\mathbf{V}}^{(0)}_{m,(m,k)}$, is then computed by performing an SVD of the stacked interfering channels $\widetilde{\mathbf{H}}_{m,(m,k)}$.

Algorithm 5 ZF for DTDD Networks performed by each $m \in \mathcal{D}$ and each $k \in \mathcal{K}_m$

1: Compute $\mathbf{V}^{(1)}_{p,(p,b)}$ from the SVD of $\mathbf{H}_{p,(p,b)} = \mathbf{U}_{(p,b)}\mathbf{\Sigma}_{p,(p,b)}\left[\mathbf{V}^{(1)}_{p,(p,b)}\mathbf{V}^{(0)}_{p,(p,b)}\right]^{\mathrm{H}}$ $\forall b \in \mathcal{K}_p$ and $\forall p \in \mathcal{U}$
2: Compute the equivalent channel $\overline{\mathbf{H}}_{m,(p,b)} = \mathbf{H}_{m,p}\mathbf{V}^{(1)}_{(p,b)}$ $\forall b \in \mathcal{K}_p$ and $\forall p \in \mathcal{U}$
3: Define $\overline{\mathbf{H}}_{m,p} = \left[\overline{\mathbf{H}}_{m,(p,1)} \quad \cdots \quad \overline{\mathbf{H}}_{m,(p,|\mathcal{K}_p|)}\right]$ $\forall p \in \mathcal{U}$
4: Define $\overline{\mathbf{H}}_m = \left[\overline{\mathbf{H}}_{m,1} \quad \cdots \quad \overline{\mathbf{H}}_{m,|\mathcal{U}|}\right]$
5: Define $\mathbf{Z}_{m,(m,k)}$ as the concatenation of $\mathbf{H}_{m,(m,b)}$ $\forall b \in \mathcal{K}_m$ and $k \neq b$
6: Define $\mathbf{T}_m$ as the concatenation of $\mathbf{H}_{m,(p,b)}$ $\forall b \in \mathcal{K}_p$, $\forall p \in \mathcal{D}$ and $p \neq m$
7: Define $\widetilde{\mathbf{H}}_{m,(m,k)} = \left[\overline{\mathbf{H}}_m \quad \mathbf{Z}_{m,k} \quad \mathbf{T}_m\right]$
8: Compute $\widetilde{\mathbf{V}}^{(0)}_{m,(m,k)}$ from the SVD of $\widetilde{\mathbf{H}}_{m,(m,k)} = \widetilde{\mathbf{U}}_{m,(m,k)}\widetilde{\mathbf{\Sigma}}_{m,(m,k)}\left[\widetilde{\mathbf{V}}^{(1)}_{m,(m,k)}\widetilde{\mathbf{V}}^{(0)}_{m,(m,k)}\right]^{\mathrm{H}}$
9: Compute $\widehat{\mathbf{V}}^{(1)}_{m,(m,k)}$ from the SVD of $\mathbf{H}_{m,k}\widetilde{\mathbf{V}}^{(0)}_{m,(m,k)} = \widehat{\mathbf{U}}_{m,(m,k)}\widehat{\mathbf{\Sigma}}_{m,(m,k)}\left[\widehat{\mathbf{V}}^{(1)}_{m,(m,k)}\widehat{\mathbf{V}}^{(0)}_{m,(m,k)}\right]^{\mathrm{H}}$
10: Define $\mathbf{W}_{m,(m,k)} = \sqrt{P_{m,(m,k)}}\left(\frac{\widetilde{\mathbf{V}}^{(0)}_{m,(m,k)}\widehat{\mathbf{V}}^{(1)}_{m,(m,k)}}{\|\widetilde{\mathbf{V}}^{(0)}_{m,(m,k)}\widehat{\mathbf{V}}^{(1)}_{m,(m,k)}\|_F}\right)$

After that, in step 9, we compute the range space $\left(\widehat{\mathbf{V}}^{(1)}_{m,(m,k)}\right)$ of the desired channel $\mathbf{H}_{m,(m,k)}$ projected into the null space of the interference, given by $\widetilde{\mathbf{V}}^{(0)}_{m,(m,k)}$ for each UE $k \in \mathcal{K}_m$.

Finally, the ZF beamforming is computed in step 10, where $P_{m,(m,k)}$ is the transmit power of AN m to UE k $\forall \in \mathcal{K}_m$.

After obtaining the ZF precoder using Algorithm 5, the interference caused by ANs in the dowlink is fully suppressed for other UEs in downlink and uplink. This method guarantees that the MRT performed by the UEs is free from cross-channel interference. The co-channel interference from other uplink UEs must still be mitigated in the AN filter, which can be done with conventional ZF or minimum mean square error (MMSE) filters.

VI. Numerical Results

In this section, we illustrate some system-level simulation results of the performance of the channel estimation and sounding signal assignment algorithms in a DTDD scenario. The simulated scenario consists of a hexagonal grid of 7 cooperative ANs, as illustrated in Figure 3.

Each cell has a radius of 200 m and each AN has four antennas, while each UE has one antenna. We assume that all links are using the same time-frequency resource, which corresponds to a reuse factor of one. To achieve higher spectral efficiency, modern systems rely on such unitary reuse, implementing more advanced techniques to cope with the interference and providing faster coordination and cooperation among cells [18]. To avoid border effects in the results we have **always obtained the estimation from cell 1**, which was in the uplink on all Monte Carlo samples. Depending on the result that is being shown, the total number of cells in uplink varies from 1 (Figure 3a) to 7 (Figure 3b), where cells are changed to uplink according to their number. That is, a result for a case where 4 cells are in uplink was obtained with cells 1-4 in uplink and cells 5-7 in downlink. Furthermore, since we intend to estimate the full channel matrix, that means that **when working in the downlink an AN has to send four different (and orthogonal) reference signals, one for each transmit antenna, while when working in the uplink the associated UE has to send only one reference signal**. Motivated by the height of the ANs, in our simulations, we considered a line-of-sight (LOS) component between all ANs as well as between an AN and a UE, but only non line-of-sight (NLOS) is considered for links between UEs. This is a simplification of the path loss model in [19], which has a probability for each link type to have a LOS component or not. The path loss models employed in our simulations are summarized in Table I [19].

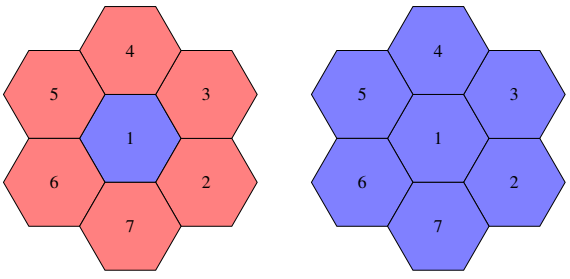

(a) Only central cell in uplink (b) All cells in uplink

Figure 3. Hexagonal grid of 7 cells.

Table I
Path loss models [19].

Link type	Path loss model
AN-to-AN	PL(R) = 98.4 + 20log$_{10}$(R), R in km
AN-to-UE	PL(R) = 103.8 + 20.9log$_{10}$(R), R in km
UE-to-UE	PL(R) = 55.78 + 40log$_{10}$(R), R in m

In this work, we consider an adaptation of the one-ring local scattering model discussed in details in [20], [21]. The one-ring channel model is widely employed when simulating MIMO systems, due to its ability to capture antenna correlation, which can affect beamforming performance. In this model, scatterers are generated inside a ring centralized at one link end (typically the receiver in a downlink transmission) [22]. Furthermore, since we are simulating a TDD system, both downlink and uplink channels are assumed to be reciprocal. That is, the channel matrix in one link direction is the transposition of the channel matrix in the other link direction. Therefore, in an AN-to-UE channel link, we only generate scatterers around UEs to obtain the downlink channel matrix and we compute its transpose to obtain the uplink channel matrix. For AN-to-AN and UE-to-UE channels the same method was adopted, where we choose one AN/UE of each channel link to place the scatterers around it.

We have analyzed the mean square error (MSE) of the channel estimation for each subcarrier, which is computed as:

$$\alpha^2_h = \frac{\mathbb{E}\left\{\left|\widehat{h} - h\right|^2\right\}}{\mathbb{E}\left\{|h|^2\right\}} \tag{10}$$

where $\widehat{h}$ is the estimated channel of a subcarrier, h is the true channel. The main simulation assumptions are summarized

Table II
SIMULATION PARAMETERS

Number of ANs	7 (Hexagonal grid)
Number of AN antennas	4
Number of UE antennas	1
Number of UEs per AN	from 1 to 6
AN and UE Transmit Power	23 dBm
Cell radius	200 m
Frequency of operation	2 GHz
Bandwidth	5 MHz
Subcarrier spacing	15 kHz
Num. estimated subcarriers	300 (all bandwidth)
Fast fading model	one-ring local scattering model [20], [21]
Angular spread (Δ)	15° [24]
Scatterers ring radius	$d \tan(\Delta)$ (distance d in meters) [20], [21]
Number of scatterers	7
Power allocation	equal power allocation (EPA)
Monte Carlo samples	1000

in Table II. The simulation parameters are equivalent to the outdoor pico environment scenario evaluated in the 3rd generation partnership project (3GPP) report [23].

The employed channel estimation method and reference signal assignment strategies are:

- **SRS**: This method is the sounding signal assignment described in Algorithm 3, which represents an LTE/NR approach where each AN allocates the sounding signals in an uncoordinated way.
- **C-SRS**: This method is the sounding signal assignment proposed in this work and described in Algorithm 4.
- **SIC**: The regular SIC channel estimation method described in Algorithm 1.
- **R-SIC**: The Refined-SIC channel estimation method proposed in this work and described in Algorithm 2.

Figures 4 and 5 illustrate the empirical cumulative distribution functions (CDFs) of the channel estimation MSE of intended and interfering channels, respectively, when all 7 ANs are operating in uplink (Figure 3b) and there are 6 UEs in each cell. This scenario is equivalent to a network where all ANs are operating in the same transmission direction (uplink or downlink), which avoids the cross-channel interference. Therefore, all interfering channels are from UEs in other cells.

From Figure 4 we can see that the worst performance is obtained with the SRS using the SIC approach, where the 50^{th} percentile in the MSE CDF is -13 dB. However, the 50^{th} percentile for the Refined-SIC estimation method achieves an MSE around -32.5 dB for SRS and -33 dB for C-SRS. This represents a gain of 20 dB in the MSE when compared with SRS with SIC. On the other hand, the gain of the C-SRS with SIC approach is only 1.4 dB better, compared with SRS with SIC. Hence, in terms of channel estimation quality, the coordination of the sounding signal assignment has no significant gains, while using the refined version of the SIC algorithm can achieve large gains.

A similar behavior could be noted in the interfering channel estimation for the same scenario, which is illustrated in Figure 5. The estimation of the interfering UE channels using the SRS and SIC algorithm achieved the worst performance and the channel estimation MSE is so high that the obtained CSI is not very useful for interference mitigation. More precisely, the 50^{th} percentile interfering channel MSE with SRS and SIC is -1.5 dB, compared to 0.4 dB, -10 dB and -10.5 dB

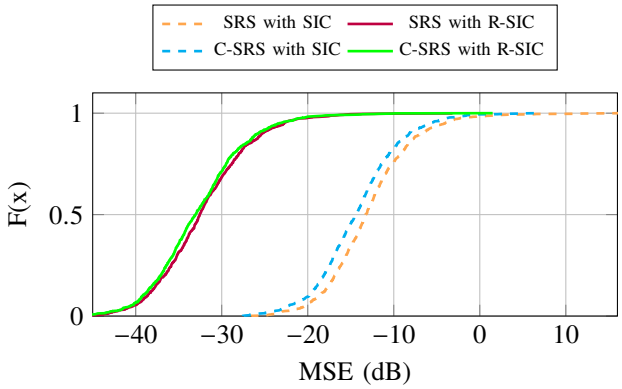

Figure 4. CDF of the MSE (in dB) quality estimation for intended channels when there are 7 ANs in uplink and 6 UEs in each cell.

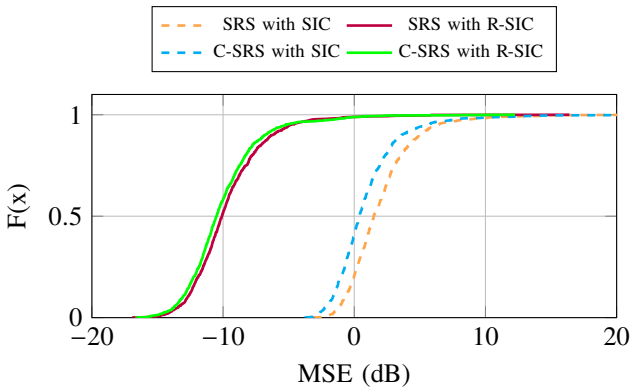

Figure 5. CDF of the interfering channel estimation MSE (in dB) when there are 7 ANs in uplink and 6 UEs in each cell.

of C-SRS with SIC, SRS with R-SIC and C-SRS with R-SIC, respectively. Considering only the case where the R-SIC algorithm is employed, we can note that the gain obtained with C-SRS compared to SRS is of around 1 dB. That is, when R-SIC is employed, the benefit of going the extra mile and coordinating the assignment of the reference signals is marginal.

We have also analyzed the 50^{th} percentile of the CDF of the channel estimation MSE for all simulated methods when the 7 ANs are operating in the uplink. In Figure 6, the 50^{th} percentile of the intended estimated channel is illustrated for a number of UEs from 1 to 6. The estimation error of the approaches employing SIC quickly increases as the number of UEs per cell increases. For all simulated system loads, the approaches with C-SRS as sounding assignment method achieved the best performance. On the other hand, the estimation error when R-SIC is employed increases with the number of UEs at a much slower rate when compared with the SIC case. Indeed, as the number of UEs increases the gap between the estimation error with SIC and R-SIC increases.

Figure 7 shows the 50^{th} percentile of the CDF of the channel estimation error of the interfering UE channels. Compared with Figure 6, the results in Figure 7 are very similar, with the only difference being the MSE values in the y axis. As expected, due to the pathloss, the MSE of the interfering UE channels is higher than the MSE of the intended channel.

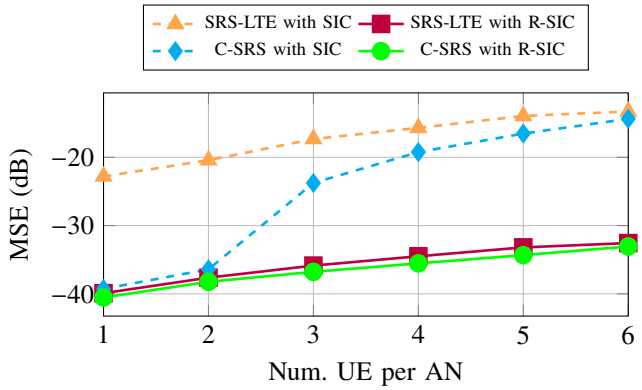

Figure 6. 50^{th} percentile of MSE CDF (in dB) of the intended channel estimation when there are 7 ANs in uplink and from 1 to 6 UEs in each cell.

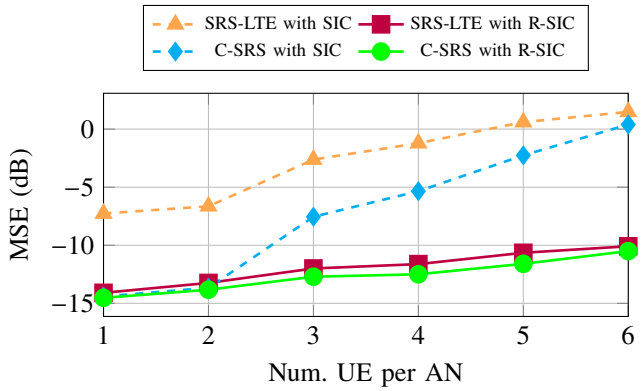

Figure 7. 50^{th} percentile of MSE CDF (in dB) of the interfering UE channels when there are 7 ANs in uplink and from 1 to 6 UEs in each cell.

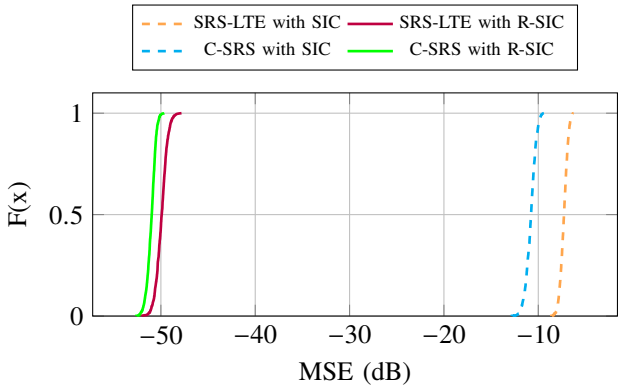

Figure 8. CDF of the interfering AN-to-AN channels when all surrounding cells are in downlink.

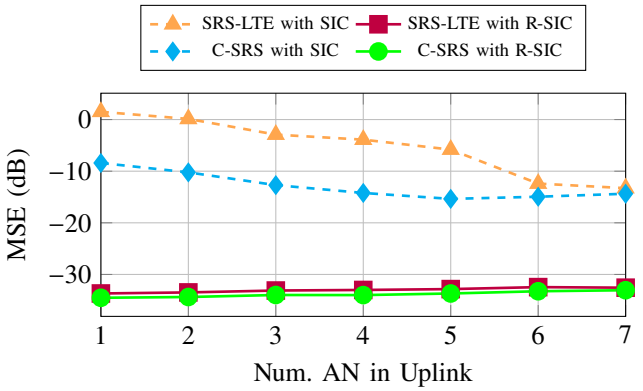

Figure 9. 50^{th} percentile of MSE CDF (in dB) of the intended UE channels with 6 UEs per cell and the number of ANs in uplink varies from 1 to 7.

In Figure 8 the channel estimation quality for the AN-to-AN channel (that is, the interfering channel) is demonstrated when 6 ANs are operating in downlink, as in Figure 3a. In this case, only the central cell is operating in uplink and performs the channel estimation. We can note in Figure 8 a large gap between the CDFs of approaches with R-SIC and SIC. If we analyze Table I, we can see that the pathloss of the AN-to-AN[7] is lower than the path loss between AN and UEs. This means that the sounding reference signal between ANs causes high interference on the sounding signal sent by UEs. That is why R-SIC, which can better mitigate these interferences, has a much higher performance gain compared to SIC in this scenario than in the previous scenario, where all ANs were in the uplink. Furthermore, due to the LOS component, the received signal power of sounding signals from ANs is much higher than the noise power, which reduces the error propagation in R-SIC and improves its performance.

In the following, we show results to analyze the impact of the number of ANs in uplink on the channel estimation. The impact on the *intended channel*[8] estimation is illustrated in Figure 9 in terms of the 5–0^{th} percentile of the MSE for all simulated approaches. The channel estimation MSE when employing SIC decreases as the number of ANs in uplink increases. However, when R-SIC is employed the error is much lower and does not change significantly with the number of ANs in the uplink. The sounding interference from surrounding ANs in downlink can be higher than the signals from desired UEs in the central AN, due to the LOS component between ANs. Also, when a surrounding AN is operating in downlink, the UEs served by it do not transmit any sounding signal and the sounding interference comes from the AN. In general, this exchange of interfering sounding source is bad for channel estimation algorithms, due to the increased interference. However, the R-SIC method performs the estimation of all received signals iteratively, improving the signal isolation in each iteration until a convergence criterion is reached. With this, the channel can be better estimated since the interference was mitigated.

Figure 10 illustrates the 50^{th} percentile of the MSE of the *interfering UE channels* when the number of ANs in uplink varies from 2 to 7[9]. For the case with 1 AN in uplink there is no interfering UE sounding signal in the system and this case is not included. The UE-AN interfering channels have larger path loss than other links and thus the error is higher than the intended channel estimation.

Based on the analyzed results, we can conclude that the approaches with R-SIC achieve the best channel estimation

[7]In this work, we considered LOS between all ANs.

[8]Channel between UEs of the central AN and the central AN.

[9]The MSE plot of the interfering AN channels is similar to Figure 10, but with much lower values in the y axis. Thus we only show the plot for interfering UE channels.

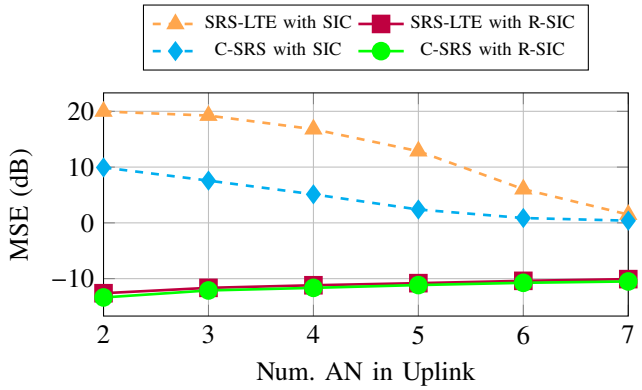

Figure 10. 50^{th} percentile of MSE CDF (in dB) of interfering UE channels with 6 UEs per cell and the number of ANs in uplink varies from 2 to 7.

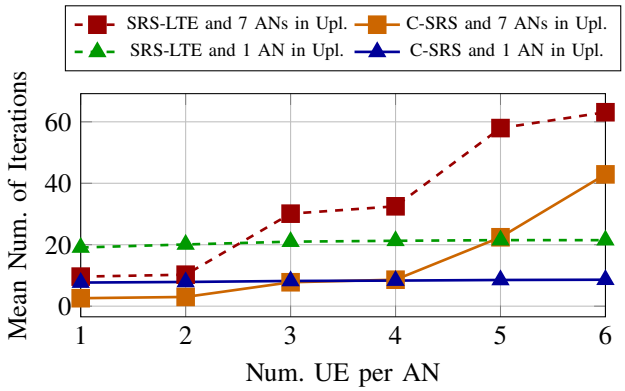

Figure 11. Mean number of iterations for the R-SIC algorithm to reach convergence for the scenario with 7 and 1 AN operating in uplink and with from 1 to 6 UEs per cell.

quality. Another conclusion is that the coordinated sounding signal distribution of C-SRS has a marginal gain in channel quality estimation when the R-SIC is performed. However, the results of methods with the SIC algorithm demonstrated gains in some loads[10] when the C-SRS is used instead of SRS.

Figure 11 illustrates the mean number of iterations for the R-SIC algorithm to reach convergence for the scenarios with 1 AN and with 7 ANs operating in uplink. We can note that the number of iterations for R-SIC convergence is reduced with C-SRS due to the interference reduction. Furthermore, when there is only one AN in uplink, with the 6 surrounding ANs operating in downlink, the number of sounding signals increases only in the uplink AN. For this reason, the mean number of iterations with one AN in uplink seems constant for all numbers of UEs per cell in Figure 11. However, the solution with C-SRS requires fewer iterations to reach the convergence than the approach with SRS-LTE. The difference in terms of the number of iterations between C-SRS and SRS is of around 13 iterations for all system loads when there is one AN operating in uplink.

On the other hand, the scenario with 7 ANs operating in uplink means that all sounding signals sent in the cooperative cluster are from UEs in the network. Therefore, when the number of UEs per cell increases, the number of sounding signals increases 7 times more. The impact of the number of sounding signals on the convergence is evident in Figure 11. In the case with 6 UEs per AN, the gap in the number of iterations is of around 20 between C-SRS and SRS-LTE. This result shows the impact on the computational complexity of R-SIC when the cell coordination is adopted in the sounding.

To assess the impact of channel knowledge on the system performance, we simulated the proposed zero-forcing beamforming described in Section V. The simulated scenario had 7 cells and one UE per cell. Due to the degrees of freedom requirement for the zero-forcing algorithm, we simulated a scenario with 8 antennas at the ANs and 1 antenna at each UE. In this way, the subspace selected by the uplink AN has rank 1. For the channel estimation, we have considered that the transmission direction in the previous TTI was opposite to the current transmission, where the sounding channel was performed. That is, the ANs that were in the uplink direction when CSI was obtained, including the central cell, are in the downlink direction when this CSI is employed to perform transmission using the proposed zero-forcing algorithm.

The channel estimation considered for the zero-forcing algorithm was performed by SRS using the proposed sounding signal assignment described in Section IV and channel estimation methods described in Section III.

For simplicity, in the reception step, we consider perfect knowledge of the channel, therefore the decoder design considers the true covariance matrix of channels and interference. We considered MMSE-interference rejection combining (IRC) as the reception filter in uplink ANs. The uplink beamforming used by UEs is the MRT based on SVD operation. This assumption removes from UEs the responsibility to reduce interference.

Let S be the number of Monte Carlo samples and C be the mean sum capacity, given by:

$$C = \frac{\sum_{s=1}^{S} \left(\sum_{\substack{k \in \mathcal{K}_m \\ \forall m \in \mathcal{U}}} \log(1 + \overleftarrow{\gamma}_{k,m}^{s}) + \sum_{\substack{k \in \mathcal{K}_m \\ \forall m \in \mathcal{D}}} \log(1 + \gamma_{m,k}^{s}) \right)}{S}, \quad (11)$$

where $\overleftarrow{\gamma}_{k,m}^{s}$ and $\gamma_{m,k}^{k}$ are the uplink and downlink SINR of sample s, respectively. Figure 12 illustrates the mean sum capacity of the zero-forcing algorithm considering the channel estimated by SRS with SIC and C-SRS with R-SIC, while the number of ANs in the uplink varies from 0 to 6.[11]

SRS-LTE with SIC and C-SRS with R-SIC are the extreme cases of sounding channel approaches with the upper and lower bound of channel estimation quality in all simulated scenarios. Therefore, the other methods are expected to reach capacity values in-between those of the simulated methods.

In Figure 12, we can perceive the impact that CSI has on beamforming performance and the corresponding gains in capacity. For 0 and 1 ANs in uplink, the gain between the estimation methods is marginal, this happens due to the low interference from UEs and few ANs in uplink. For the scenarios from 2 to 6 ANs in uplink, the amount of interference increases

[10]Number of UEs per cell.

[11]That is, when the number of cells in uplink direction during CSI acquisition changes from 7 to 1.

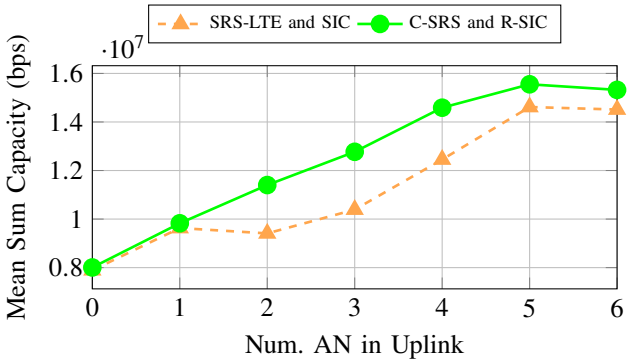

Figure 12. Mean system sum capacity of proposed zero-forcing beamforming when SRS-LTE with SIC and C-SRS with R-SIC approaches are used.

due to the LOS between ANs. In these scenarios, the zero-forcing mitigates the cross-interference, impacting the system capacity, and the better the estimated channels, the better this mitigation will be.

VII. Conclusions

In this work, we have investigated the quality of the channel estimation in a DTDD scenario, as well as the corresponding performance gains depending on the quality of the available channel state information. In the simulated scenario, when the number of uplink ANs increases, the quality of the channel estimation increases. This happens due to LOS between ANs, which is somewhat an extreme case, but is reasonable to assume that the path loss coefficient of the AN-to-AN channels is lower than the AN-to-UE channels. Nevertheless, with the proposed Refined-SIC algorithm, the channel estimation mean square error was low enough to be useful even when most of the ANs are in the downlink.

We have also investigated the possible gains with coordination between ANs in the sounding signal assignment. For SRS and DMRS, the amount of fully orthogonal sounding signals are limited by the number of comb patterns/OCCs and cyclic shifts. Differently from the ANs in the LTE standard, which assign these resources in an uncoordinated way, we propose a new sounding signal assignment algorithm that coordinates the orthogonal sounding signals between ANs to reduce the sounding interference. Our simulations have shown that the coordination can improve the sounding quality when the SIC algorithm is adopted as the channel estimation method. On the other hand, most of these gains can be obtained by simply using our proposed R-SIC channel estimation algorithm, without any coordination. The advantage of also using coordination along with the R-SIC channel estimation algorithm is reducing the complexity of the R-SIC algorithm, since it will require fewer iterations to converge. Hence, there is a trade-off between computational complexity and communication overhead between ANs, which should be considered.

Another contribution of this work is the zero-forcing beamforming to DTDD networks. In DTDD networks, where we have AN-to-AN interference, there is a lack of degrees-of-freedom to perform zero-forcing beamforming and mitigate the cross-interference. The proposed beamforming algorithm solves this issue by selecting a subspace for each AN, based on the channels of that AN's UEs. Our numerical results have shown that the CSI quality can improve the performance of the proposed algorithm.

References

[1] A. Lozano, R. W. Heath, and J. G. Andrews, "Fundamental limits of cooperation," *IEEE Transactions on Information Theory*, vol. 59, no. 9, pp. 5213–5226, Sep. 2013. DOI: 10.1109/TIT.2013.2253153.

[2] H. Kim, J. Kim, and D. Hong, "Dynamic TDD systems for 5G and beyond: A survey of cross-link interference mitigation," *IEEE Communications Surveys Tutorials*, pp. 1–1, 2020, early access. DOI: 10.1109/COMST.2020.3008765.

[3] 3GPP, *Evolved Universal Terrestrial Radio Access (E-UTRA), Physical channels and modulation*, Release 11 TR 36.211, Dec. 2012.

[4] ——, *TS 38.211 5G NR Physical channels and modulation*, Release 15 TS 38.211, Jul. 2018.

[5] L. R. Costa, D. C. Moreira, S. Sandberg, A. Simonsson, and Y. C. B. Silva, "Interference mitigation based on precoded SRS," in *Proc. IEEE Sensor Array and Multichannel Signal Processing Workshop (SAM)*, Jul. 2016, pp. 1–5. DOI: 10.1109/SAM.2016.7569712.

[6] L. Nasraoui and L. N. Atallah, "SRS-based D2D neighbor discovery scheme for LTE cellular networks," in *Proc. IEEE International Symposium on Personal, Indoor, and Mobile Radio Communications (PIMRC)*, Oct. 2017, pp. 1–5. DOI: 10.1109/PIMRC.2017.8292531.

[7] E. Hong, J. Baek, and G. Kaddoum, "A study on channel estimation algorithm with sounding reference signal for tdd downlink scheduling," in *Proc. IEEE International Symposium on Personal, Indoor and Mobile Radio Communications (PIMRC)*, Oct. 2017, pp. 1–6. DOI: 10.1109/PIMRC.2017.8292249.

[8] Q. Zhang, Y. Chang, and T. Zeng, "SRS limited user grouping scheduling algorithm for downlink massive MIMO systems," in *Proc. IEEE Wireless Communications and Networking Conference (WCNC)*, Apr. 2019, pp. 1–6. DOI: 10.1109/WCNC.2019.8885621.

[9] L. G. Giordano, L. Campanalonga, D. López-Pérez, A. Garcia-Rodriguez, G. Geraci, P. Baracca, and M. Magarini, "Uplink sounding reference signal coordination to combat pilot contamination in 5G massive MIMO," in *Proc. IEEE Wireless Communications and Networking Conference (WCNC)*, Apr. 2018, pp. 1–6. DOI: 10.1109/WCNC.2018.8377316.

[10] K. Ardah, Y. C. B. Silva, W. C. Freitas, F. R. P. Cavalcanti, and G. Fodor, "An ADMM approach to distributed coordinated beamforming in dynamic TDD networks," in *Proc. IEEE International Workshop on Computational Advances in Multi-Sensor Adaptive Processing (CAMSAP)*, Dec. 2017, pp. 1–5. DOI: 10.1109/CAMSAP.2017.8313195.

[11] L. R. Costa, D. C. Moreira, Y. C. B. Silva, W. C. Freitas, and F. R. M. Lima, "User grouping based on spatial compatibility for dynamic-TDD cooperative networks," in *Proc. IEEE Global Communications Conference (GLOBECOM)*, Dec. 2018, pp. 1–6. DOI: 10.1109/GLOCOM.2018.8647677.

[12] E. de Olivindo Cavalcante, G. Fodor, Y. C. B. Silva, and W. C. Freitas, "Distributed beamforming in dynamic TDD MIMO networks with BS to BS interference constraints," *IEEE Wireless Communications Letters*, vol. 7, no. 5, pp. 788–791, Oct. 2018, ISSN: 2162-2345. DOI: 10.1109/LWC.2018.2825330.

[13] ——, "Bidirectional sum-power minimization beamforming in dynamic TDD MIMO networks," *IEEE Transactions on Vehicular Technology*, vol. 68, no. 10, pp. 9988–10 002, Oct. 2019, ISSN: 1939-9359. DOI: 10.1109/TVT.2019.2937474.

[14] P. Komulainen, A. Tölli, and M. Juntti, "Effective CSI signaling and decentralized beam coordination in TDD multi-cell MIMO systems," *IEEE Transactions on Signal Processing*, vol. 61, no. 9, pp. 2204–2218, May 2013, ISSN: 1053-587X. DOI: 10.1109/TSP.2013.2247597.

[15] S. Lagen, A. Agustin, and J. Vidal, "Decentralized beamforming with coordinated sounding for inter-cell interference management," in *Proc. European Wireless Conference*, May 2014, pp. 305–310.

[16] P. Bertrand, "Channel Gain Estimation from Sounding Reference Signal in LTE," in *Proc. IEEE Vehicular Technology Conference (VTC)*, vol. 73, Budapest, Hungary, May 15–18, 2011. DOI: 10.1109/VETECS.2011.5956571.

[17] D. Chu, "Polyphase codes with good periodic correlation properties (corresp.)," *IEEE Transactions on Information Theory*, vol. 18, no. 4, pp. 531–532, Jul. 1972, ISSN: 0018-9448. DOI: 10.1109/TIT.1972.1054840.

[18] B. Clerckx and C. Oestges, "Chapter 13 - Multi-Cell MIMO," in *MIMO Wireless Networks (Second Edition)*, B. Clerckx and C. Oestges, Eds., Academic Press, 2013, pp. 525–596, ISBN: 978-0-12-385055-3. DOI: 10.1016/B978-0-12-385055-3.00013-4. [Online]. Available: http://www.sciencedirect.com/science/article/pii/B9780123850553000134.

[19] 3GPP, "R1-120948: Simulation assumptions for multi-cell scenarios for TDD IMTA," 3GPP, Technical Report, Feb. 2012.

[20] A. Adhikary, J. Nam, J. Y. Ahn, and G. Caire, "Joint spatial division and multiplexing - the large-scale array regime," *IEEE Transactions on Information Theory*, vol. 59, no. 10, pp. 6441–6463, Oct. 2013. DOI: 10.1109/TIT.2013.2269476.

[21] M. Pätzold, *Mobile Radio Channels*. Wiley, 2012, ISBN: 9780470517475.

[22] A. Abdi and M. Kaveh, "A space-time correlation model for multielement antenna systems in mobile fading channels," *IEEE Journal on Selected Areas in Communications*, vol. 20, no. 3, pp. 550–560, 2002.

[23] 3GPP, "TR-36.828 v11.0.0. further enhancements to LTE time division duplex TDD for downlink-uplink (DL-UL) interference management and traffic adaptation," 3GPP, Technical Report, Jun. 2012.

[24] J. Nam, A. Adhikary, J.-Y. Ahn, and G. Caire, "Joint Spatial Division and Multiplexing: Opportunistic Beamforming, User Grouping and Simplified Downlink Scheduling," *IEEE Journal of Selected Topics in Signal Processing*, vol. 8, no. 5, pp. 876–890, Oct. 2014. DOI: 10.1109/JSTSP.2014.2313808.

Darlan. C. Moreira received B.Sc. degree in electrical engineering in 2005 from the Federal University of Ceará (UFC), Fortaleza, Brazil, in 2005. In 2007 and 2020 he received the M.S. and Ph.D. degrees, respectively, in Teleinformatics Engineering from the same institution. In 2007, he visited Ericsson Research in Kista, Sweden, for 3 months. In 2010, he visited Supélec in Gif-sur-Yvette, France, for 6 months. Since 2005 he has been a researcher at Wireless Telecommunications Research Group (GTEL), Brazil, where he has been working in projects within the technical cooperation between GTEL and Ericsson Research. Some topics of his research interests include machine learning, MIMO transceiver design, channel estimation, interference management and modeling and simulation of cellular communication.

László R. da Costa received the B.Sc. degree in Computer Engineering from Federal University of Ceará (UFC), Sobral, Brazil, in 2014 and the M.Sc. degree in Computer and Electrical Engineering from Federal University of Ceará (UFC), Sobral, Brazil, in 2016. He is currently pursuing D.Sc. degree in Telecommunications Engineering from the Federal University of Ceará, Fortaleza, Brazil. In 2019, he has been in an internship at Technische Universität Darmstadt (TUD), Germany. He is also a researcher at Wireless Telecom Research Group (GTEL), Fortaleza, Brazil, where he works in projects in cooperation with Ericsson Research. His research interests include radio resource management, numerical optimization, and multiuser/multiantenna communications.

Yuri C. B. Silva received the B.Sc. and M.Sc. degrees from the Federal University of Ceará, Fortaleza, Brazil, in 2002 and 2004, respectively, and the Dr.-Ing. degree from the Technische Universität Darmstadt, Germany, in 2008, all in Electrical Engineering. From 2001 to 2004 he was with the Wireless Telecom Research Group (GTEL), Fortaleza, Brazil. In 2003 he was a visiting researcher at Ericsson Research, Stockholm, Sweden. From 2005 to 2008 he was with the Communications Engineering Lab of the Technische Universität Darmstadt. He is currently an Associate Professor at the Federal University of Ceará and researcher at GTEL. He also holds a productivity fellowship in technological development and innovation from CNPq. His main research interests are in the areas of wireless communications systems, multi-antenna processing, interference management, multicast services, and cooperative communications.

Igor M. Guerreiro received the B.S., M.S. and Ph.D. degrees in Teleinformatics Engineering from the Federal University of Ceará (UFC), Brazil, in 2007, 2010 and 2016, respectively. He currently holds a post-doc position at the UFC Department of Teleinformatics Engineering. Since 2007 he has been a researcher at Wireless Telecommunications Research Group (GTEL), Brazil, working in research projects within a technical cooperation with Ericsson Research, Sweden. In 2008, he was a guest researcher at Virginia Tech Advanced Research Institute (ARI), Arlington, Virginia, USA. Before starting the Ph.D. course at UFC, he visited Ericsson in 2010 in Luleå, Sweden, for 5 months, and another time in San José, California, USA, for 3 months. As a Ph.D. student, he visited both Ericsson and the Royal Institute of Technology (KTH) in 2014-15 in Stockholm, Sweden, for a year-long period. Some topics of his research interests include techniques for MIMO transceiver design, distributed optimization and machine learning for wireless communication systems, modeling and simulation of cellular communication, dynamic spectrum access methodologies, physical layer aspects for Internet of Things.